Three-Dimensional Confinement in the Conduction Band Structure of InP

C. S. Menoni, L. Miao, and D. Patel

Department of Electrical and Computer Engineering, Colorado State University, Fort Collins, Colorado 80523-1373

O. I. Mic'ic' and A. J. Nozik

National Renewable Energy Laboratory, Golden, Colorado 80401-3393

Strong quantum confinement in InP is observed to significantly reduce the separation between the direct and indirect conduction band states. The effects of three-dimensional confinement are investigated by tailoring the initial separation between conduction band states using quantum dots (QDs) of different sizes and hydrostatic pressure. Analyses of the QD emission spectra show that the X_{1c} states are lowest in energy at pressures of ~6 GPa, much lower than in the bulk. The transition to the X_{1c} states can be explained by either a sequence of Γ-L and L-X crossings, or by the crossover between strongly coupled Γ and X states.

Quantum confinement has dramatic effects on the optical and electronic properties of semiconductors. Quantum confinement gives rise to electron states whose energy can be varied with the confinement dimensions, and dramatically changes the density of states from steplike in one-dimensionally confined quantum well systems to atomiclike in three-dimensionally confined quantum dots (QDs). The changes in the density of states and the possibility of tailoring the band gap have attracted attention for the application of quantum confined systems in the design of optoelectronic devices.

In zinc blende quantum well structures, quantum confinement has also been found to alter the electronic structure. Increased carrier confinement leads to (i) an electronic configuration in which multiple quantum wells (MQWs) of direct band-gap semiconductors become intrinsically indirect, i.e., L_{1c} or X_{1c} are the lowest conduction band states in the well, or (ii) a type II conduction band alignment with the lowest indirect conduction band state located in the barrier and the highest valence band state in the well. The former case is obtained in InGaP/InAlP MQWs and the latter is observed in GaAs/AlAs MQWs for well widths less than 35 Å [1,2].

In three-dimensionally confined systems, model calculations predict quantum confinement to significantly alter the electronic structure of zinc blende semiconductors as the lower effective mass Γ_{1c} state rises to higher energy much faster than the higher effective mass L_{1c} and X_{1c} states [3,4]. In strained III-V QDs grown epitaxially, the interplay between carrier confinement and strain could result in either a type II electronic configuration with X_{1c}-derived states in the capping layer and holes in Γ_{1v}-derived QD states, or in a type I configuration where the indirect states in the QD are lowest in energy [4]. Instead, in freestanding colloidal QDs, only an intrinsically indirect electronic configuration is possible [3,5]. The model calculations predict Γ-X transitions to be observed in freestanding GaAs QDs with diameter <40 Å [6], and in InP QDs at pressures

around 7 GPa, as confinement alone is not sufficient to lower the X-like states below Γ-like states even for zero dimension [3].

In this Letter, we present the first experimental evidence showing that strong quantum confinement significantly reduces the separation between direct and indirect conduction band states in InP. To determine the effects of three-dimensional confinement, we used QDs of different size to tailor the initial separation among Γ_{1c}-, L_{1c}-, and X_{1c}-like states and, in addition, applied hydrostatic pressure to further modify the electronic structure and reveal the indirect states at high pressures. Since in bulk III-V materials Γ_{1c}, L_{1c}, and X_{1c} shift at characteristics rates of ~80 meV/GPa, ~50 meV/GPa, and ~−10 meV/GPa, respectively, the pressure rate of change of the emission peak (dE_p/dp) has been used as a signature for identifying the direct and indirect states [7].

The colloidally grown InP QDs were synthesized from a mixture of indium trichloride, tris-(trimethylsilyl)phosphine [P(SiMe$_3$)$_3$], trioctylphosphine oxide (TOPO), and trioctylphosphine (TOP) at room temperature and then heated at high temperature [8,9]. The resulting InP QD samples consisted of InP nanocrystals that crystallize in the zinc blende structure, and whose surface was capped by TOPO [8,9]. The QDs were further etched in a methanolic solution of HF that passivates the surface, enhancing the InP band edge emission and reducing the sub-band-gap emission associated with surface states [8]. Selective precipitation of the QD solution was used to obtain three different samples with mean QD diameters $\langle d \rangle$ of 32, 35, and 56 Å, respectively, and standard deviation $\langle \sigma_d \rangle = 10\%$.

For the high pressure experiments, the InP QDs were spun over a thin (<50 μm) piece of InP bulk (Zn-doped, $p = 5 \times 10^{17}$ cm^{-3}) and loaded into the pressure chamber of a diamond anvil cell. A second InP bulk sample also loaded in the chamber was used to track the emission of bulk InP at different pressures and to perform a background subtraction which considerably improved the

QD signal to noise ratio at high pressures, where it became very weak. The two samples, and a ruby chip used to monitor the pressure, were surrounded by solid argon which served as the pressure transmitting medium and allowed hydrostatic conditions to reach pressures in excess of 7 GPa. The changes in the electronic structure of the QDs and bulk InP were monitored from the shift of the photoluminescence (PL) emission excited by the 410 nm output from a frequency doubled Ti:sapphire laser. The emission was collected and analyzed using a spectrometer and liquid nitrogen cooled charge-coupled device detector.

Typical emission spectra for the 32 Å QDs at different pressures is shown in Fig. 1(a). At atmospheric pressure, the spectra is composed of a PL peak at 1.95 eV which corresponds to the band-to-band (BB) emission and a second emission peak at 1.7 eV which originates from surface states (SS) associated with surface defects [5,8,10,11]. Fitting Gaussian functions to the spectra allowed the determination of the peak energy, integrated intensity, and full width at half maximum (FWHM) of each emission band. The BB-PL emission is broad with a FWHM ~150 meV, reflecting the size distribution of the colloidally grown InP QDs. The BB-PL peak energy blueshifts with pressure initially at a rate $dE_p/dp \sim 80$ meV/GPa, slightly larger than that measured in bulk InP ($dE_p/dp = 65$ meV/GPa). At higher pressures, dE_p/dp decreases and becomes slightly negative above 6 GPa, as shown in Fig. 2(a). Above 7 GPa, the QD BB emission is basically quenched. The BB-PL peak behavior is completely reversible as shown by the open symbols in Fig. 2(a). The changes in dE_p/dp are also accompanied by changes in the PL intensity and FWHM, shown in Fig. 2(b). The PL intensity is almost constant to ~2 GPa where it starts to decrease and reaches a value ~2 orders of magnitude smaller than its atmospheric pressure value at the highest pressure. The FWHM increases by 50% over the whole pressure range; however, its change is more prominent above 4 GPa. The SS PL, 300 meV below the BB emission, also blueshifts but at a lower rate; dE_p/dp also decreases with pressure,
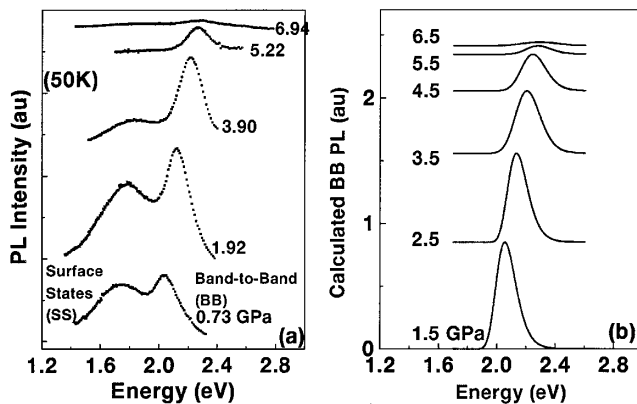
undertracking the behavior of the BB emission. The lower value of dE_p/dp in the SS emission compared to the BB emission is not surprising as these are deep states which are generally less sensitive to pressure. The SS also disappears when the main BB emission quenches at ~7 GPa.

The BB-PL behavior just described for the 32 Å QD sample is also observed in the 35 and 56 Å QDs, as shown in Fig. 3. The most obvious difference in the pressure behavior of the QDs compared to bulk InP is the bowing of the BB-PL peak energy with pressure which contrasts with the linear behavior of the bulk InP over the same pressure range. The bowing in the QD data arises from changes in dE_p/dp which reduces from ~80 to ~40 meV/GPa at ~3 GPa and becomes constant or slightly negative with pressure at ~6 GPa in the 32 and 35 Å samples. In the 56 Å QD sample, dE_p/dp changes from 75 to 40 meV/GPa at 4 GPa. The second decrease in dE_p/dp is not observed as the emission is quenched at lower pressures than in the smaller QD samples. At the onset of the first change in dE_p/dp, the BB-PL intensity starts to decrease, and markedly reduces at ~6 GPa when the second change in dE_p/dp occurs. The decrease in dE_p/dp and BB-PL intensity with pressure are signatures
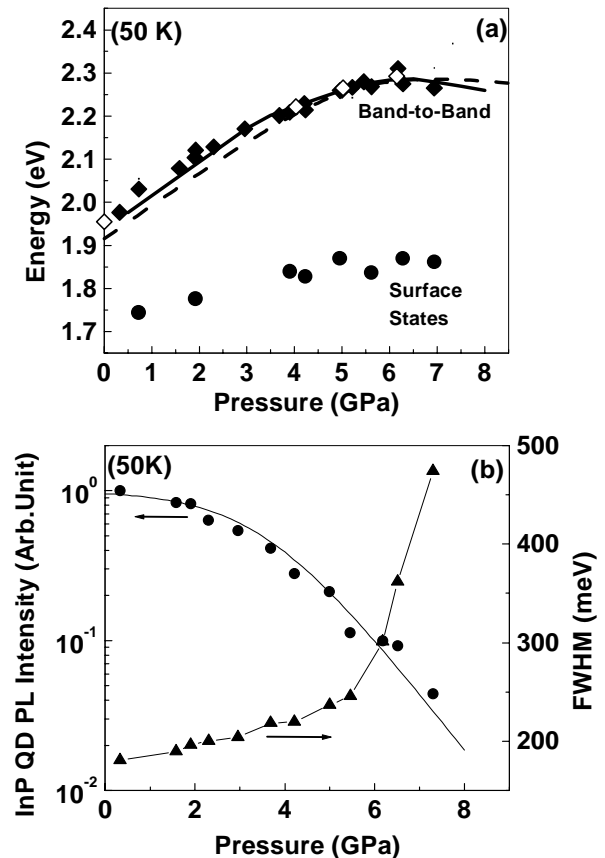

FIG. 2. (a) Variation of the BB-PL and SS-PL peak energy for 32 Å InP QDs; solid symbols (◆): upstroke; open symbols (◇): downstroke. The dotted and solid lines are the results of a fit with a simulation that considers Γ-X transfer and Γ-L-X transfer, respectively. (b) Pressure dependence of the integrated BB-PL emission (●) and FWHM (▲).

FIG. 1. (a) Emission spectra of 32 Å InP QDs at different pressures. (b) Simulated BB emission obtained when a sequence of Γ-L-X transitions occur at high pressure.

of carrier transfer to indirect conduction band states. The initial change in dE_p/dp could be interpreted as being due to a Γ-L transition, and the second change could result from an L-X transition. The significant reduction in the PL intensity at ~6 GPa is also a strong indication of carrier transfer to the lower oscillator strength indirect X_{1c} states. But the band crossing behavior and associated intensity changes of InP QDs may be more complex than just described, depending on the strength of Γ-L-X intervalley mixing. In the presence of intervalley mixing, the conduction band states near a transition show an anticrossing behavior which is reflected in hydrostatic pressure experiments as a splitting of optical transitions and smearing out of their pressure dependence [12,13]. De-

pending on the strength of the mixing, the QD peak emission energy shift with pressure could significantly depart from the bulk behavior. The overall intensity profile of the ensemble QD PL emission should also be considerably modified. Γ-L-X mixing, coupled with the considerable reduction in the emission efficiency of X_{1c}-like states, may prevent the observation of a pure X-like behavior in InP QDs.

To visualize the behavior of the QD PL peak energy with pressure, we simulated the QD emission and tracked the position of its peak at different pressures. The ensemble PL emission intensity was obtained by superimposing the single-dot emission of a collection of QDs of diameter d, average diameter $\langle d \rangle$, and standard deviation σ_d, which follows a Gaussian distribution in dot size [10]:

$$\overline{I_{\text{PL}}}(E, E_{\text{exc}}, \langle d \rangle, p) = \sum_{d > d_c(E_{\text{exc}})} \alpha(E_{\text{exc}}, d) \left[\frac{A(p)}{\sqrt{2\pi}\,\sigma_{\text{PL}}} e^{\{E - [E_g(d,p) - \Delta(d)]^2\}/(2\sigma_{\text{PL}}^2)} \right] \left[\frac{1}{\sqrt{2\pi}\,\sigma_d} e^{(d - \langle d \rangle)^2/(2\sigma_d^2)} \right]. \quad (1)$$

In the single-dot emission, $E_g(d, p)$ is the excitonic band-gap energy, σ_{PL} is the intrinsic broadening, and $\Delta(d)$ is the single-dot redshift which varies with d as $\Delta(d) = 9.5/d^{1.96}$, where d is expressed in units of Å [10]. $\alpha(E_{\text{exc}}, d)$ is the single-dot absorption coefficient at the excitation energy E_{exc}, and depends on dot diameter as $\alpha \sim (a_B/d)^3$, where a_B is the Bohr radius. The sum over d in Eq. (1) is limited to those values satisfying the condition $E_g(d) < E_{\text{exc}}$, which is our case at all pressures for all three samples. $A(p)$ is the amplitude which was

FIG. 3. Variation of the BB-PL peak with pressure for 32 Å (◆), 35 Å (■), and 56 Å (●) InP QDs and InP bulk (▲). The arrows indicate the pressures at which dE_p/dp changes in the QDs. The solid lines are obtained from the fit of the data with the Γ-L-X simulation.

adjusted at atmospheric pressure to match the measured BB emission. The dependence of the Γ_{1c}-like E_g on dot size was taken equal to $1.42 + 15.10/d^{0.93}$ [5].

To model the pressure behavior of the ensemble PL, we first considered that only a Γ-X transition takes place. The pressure dependence was incorporated in the single-dot excitonic band gap E_g, which varies with pressure as

$$E_g(p) = E^- = E(P_c) + \frac{1}{2}(\alpha_\Gamma + \alpha_X)(p - P_c)$$
$$- \{[\frac{1}{2}(\alpha_\Gamma - \alpha_X)(p - P_c)]^2 + V_{\Gamma X}^2\}^{1/2}. \quad (2)$$

$E_g(p)$ given in Eq. (2) is obtained from first order perturbation theory when two states, Γ and X in this case, interact or become mixed near a critical pressure P_c [12]. α_Γ and α_X in Eq. (2) are the pressure coefficients of the unperturbed Γ_{1c} and X_{1c} states, away from P_c. $E(P_c)$ is the energy at which the unperturbed states would cross; i.e., $E_\Gamma(P_c) = E_X(P_c)$ and $V_{\Gamma X}$ is the interaction or mixing potential. In our simulation, α_Γ was elected to be the value of dE_p/dp measured close to atmospheric pressure, and α_X was set equal to -16 meV/GPa, a typical value for the X pressure coefficient, and equal to that measured in InAs/GaAs QDs [1,12,14]. Using α_Γ, α_X, and considering the X-excitonic band-gap energy to vary with dot size as $E_X^{\text{dot}} = 2.3 + 135.8992/d^{1.7165}$ [15], P_c was calculated for each dot size within the ensemble. For QDs of $\langle d \rangle = 32$ and 35 Å, P_c equals 6.2 and 6.5 GPa, respectively [3], very close to the experimental value at which dE_p/dp is found to be pressure independent. Since P_c is size dependent, near the Γ-X crossover the PL emission is composed of the emission from larger single dots whose conduction ground state is Γ_{1c}-like and smaller ones in which X_{1c}-like states are the lowest. To account for the superposition of markedly different emission states, we set in our simulation the peak amplitude of the X_{1c}-like states
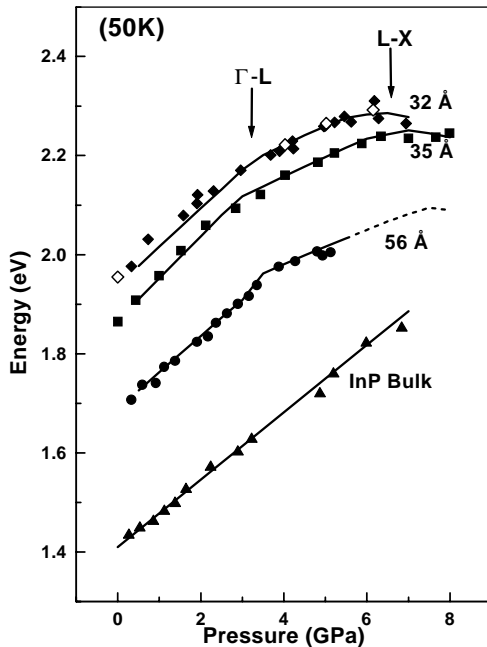
to be 2 orders of magnitude smaller than that of Γ_{1c}-like states, following the trend observed in the experiments. In the pressure dependence of Eq. (1), we also considered the effect of state mixing in the excitonic binding energy, which was calculated semiempirically from the binding energy of the Γ-like states taken to be equal to $\Delta(d)$ [16]. Leaving $V_{\Gamma X}$ as an undetermined parameter, we calculated the emission spectrum at different pressures [Fig. 1(b)], and fitted its peak energy variation with pressure to the experimental data for all three samples. The results of the least squares fit, shown by the dotted line in the 32 Å data of Fig. 2(a), yield $V_{\Gamma X} = 70$ meV. This large value of $V_{\Gamma X}$ gives the band-gap dependence on pressure the sublinear behavior observed in the experiment. It also perturbs the Γ_{1c}-like band gap close to atmospheric pressure, lowering $E_g \sim 0.04$ eV below the measured value, and predicts a pure X_{1c}-like behavior to occur well beyond 7 GPa. However, it should be noted that, since $V_{\Gamma X}$ was obtained by setting P_c for each dot in the ensemble at ~ 6 GPa, its value represents an upper limit. This choice coupled with the uncertainty in α_X (which for the InP QDs cannot be directly measured as a pure X-like behavior is not observed) are likely to be responsible for the difference between the value of $V_{\Gamma X}$ determined from our analysis and that predicted by model calculations [3].

We also considered in our simulation the possibility of a Γ-L crossing at lower pressures followed by an L-X crossing at higher pressures. This scenario is possible in the QDs as the L_{1c}-like states lie below X_{1c} at atmospheric pressure [5], provided the Γ-L separation decreases faster than Γ-X. A Γ-L-X sequence of electronic transitions would produce changes in dE_p/dp similar to those observed experimentally. The Γ-L transition was incorporated in the simulation by calculating E_g in Eq. (2) assuming the unperturbed Γ_{1c} and L_{1c} states cross at a critical pressure P_{cL} of 3.3, 3.0, and 3.6 GPa equal to that where the first change in dE_p/dp is observed in the 32, 35, and 56 Å QDs, respectively. α_L was set equal to $dE_p/dp = 40$ meV/GPa, the slope of the experimental data between 3 and 6 GPa. Selecting P_{cL} and α_L for all three samples was equivalent to determining the variation of the excitonic band gap with QD diameter as was done in the Γ-X simulation. α_Γ, α_X, and the Γ-X separation at atmospheric pressure were kept the same as in the previous case; thus, Eq. (2) modeled the L-X crossing around 6 GPa where dE_p/dp becomes independent of pressure. The solid lines in the data of Figs. 2(a) and 3 show the results of the fit when Γ-L and L-X transfer occur. Since the bowing in the emission peak behavior is mainly accounted for by the changes in dE_p/dp, the intervalley mixing potentials obtained from the fit $V_{\Gamma L} = 2$ meV and $V_{LX} = 10$ meV are smaller and comparable to those calculated in Ref. [3], and measured in InAs/GaAs QDs [12].

The above results undoubtedly show that a transition to X_{1c}-like states occurs in InP QDs at ~ 6 GPa, much lower than in bulk InP [17], reflecting the effects of quantum confinement on the electronic structure predicted by theory [3]. However, the detailed nature of this transition is not uniquely established, as a pure Γ, L, and X pressure behavior is not distinct in the freestanding InP QDs. This is because, near a crossover, the ensemble emission is composed of the single-dot emission from larger $(d > \langle d \rangle)$ and smaller $(d < \langle d \rangle)$ QDs whose conduction ground states have markedly different pressure behavior. Γ-L-X intervalley mixing even further modifies the collective pressure dependence of the emission. Accounting for these effects, the transition to X_{1c} states can be explained as a Γ-L crossover followed by an L-X crossover if the changes in dE_p/dp are used as a signature of the Γ_{1c}, L_{1c}, and X_{1c} states, or by the crossing of strongly mixed Γ_{1c} and X_{1c} states. Nevertheless, in any case, the 2 orders of magnitude reduction in the integrated intensity at ~ 6 GPa is a strong indication of carrier transfer to the X_{1c} states which are lowest in energy at the highest pressures.

[1] D. Patel, K. Interholzinger, P. Thiagarajan, G. Y. Robinson, and C. S. Menoni, Phys. Rev. B **53**, 12 633 (1996).
[2] K. Meissner et al., Appl. Phys. Lett. **59**, 259 (1991).
[3] H. Fu and A. Zunger, Phys. Rev. Lett. **80**, 5397 (1998).
[4] A. Franceschetti and A. Zunger, Phys. Rev. B **52**, 14 664 (1995).
[5] H. Fu and A. Zunger, Phys. Rev. B **56**, 1496 (1997).
[6] A. Franceschetti and A. Zunger, Appl. Phys. Lett. **68**, 3455 (1996).
[7] I. L. Spain, Contemp. Phys. **28**, 523 (1987).
[8] O. I. Micic, C. J. Curtis, K. M. Jones, J. R. Sprague, and A. J. Nozik, J. Phys. Chem. **98**, 4966 (1994).
[9] O. I. Micic et al., J. Phys. Chem. **99**, 7754 (1995); O. I. Micic, J. Sprague, Z. Lu, and A. J. Nozik, Appl. Phys. Lett. **68**, 3150 (1996).
[10] O. I. Micic et al., J. Phys. Chem. **101**, 4904 (1997).
[11] A stronger contribution of the SS emission in the 32 Å sample is observed in these experiments because the sample was not pretreated with an HF solution immediately before loading.
[12] G. H. Li, A. R. Goñi, K. Syassen, O. Brandt, and K. Ploog, Phys. Rev. B **50**, 18 420 (1994).
[13] W. Shan et al., Phys. Rev. Lett. **82**, 1221 (1999).
[14] D. J. Wolford and J. A. Bradley, Solid State Commun. **53**, 1069 (1985).
[15] H. Fu (private communication).
[16] The pressure dependent exciton binding energy was calculated as $\Delta_{\Gamma X} = \Delta(d) [\mu(p)/\mu(p = 0)]$, where $\mu(p)$ is the exciton reduced effective mass. The functional dependence of $\mu(p)$ on $V_{\Gamma X}$ and $E_g(p)$ is the same as given in Eq. (8) of Ref. [12]. At $p = 0$, $\mu_\Gamma = 0.07 m_0$, and $\mu_X = 0.144 m_0$ for the Γ and X states, respectively.
[17] S. Ernst, A. R. Goñi, K. Syassen, and M. Cardona, Phys. Rev. B **53**, 1287 (1996).